Tight Binding Inhibitors of Scytalone Dehydratase: Effects of Site-Directed Mutations

Douglas B. Jordan,*,‡ Gregory S. Basarab,§ James J. Steffens,|| Rand S. Schwartz,|| and James G. Doughty‡

DuPont Pharmaceuticals Company, Experimental Station, Route 141 and Henry Clay Road, Wilmington, Delaware 19880-0400, DuPont Central Research and Development, Experimental Station, Wilmington, Delaware 19880, and DuPont Agricultural Products, Experimental Station, Wilmington, Delaware 19880

Received February 29, 2000; Revised Manuscript Received May 9, 2000

ABSTRACT: We explore the use of site-directed mutations of scytalone dehydratase to study inhibitor binding interactions. The enzyme is the physiological target of new fungicides and the subject of inhibitor design and optimization. X-ray structures show that potent inhibitors (K_i's $\approx 10^{-11}$ M) interact mostly with 11 amino acid side chains and, in some cases, with a single backbone amide. Fifteen site-directed mutants of the 11 enzyme residues were prepared to disrupt enzyme−inhibitor interactions, and inhibition constants for 13 inhibitors were determined to assess changes in binding potencies. The results indicate that two of the six hydrogen bonds (always present in X-ray structures of native enzyme−inhibitor complexes) are not important for inhibitor binding. The other four hydrogen bonds are important for inhibitor binding, and the strength of the individual bonds is inhibitor-dependent. Inhibitor atoms remote from the hydrogen bonds influence their strength, presumably by effecting small changes in inhibitor orientation. Several hydrophobic amino acid residues are important recognition elements for lipophilic inhibitor functionalities, which is fully consistent with X-ray structures determined from crystals of enzyme−inhibitor complexes grown at neutral pH but not with those determined from crystals grown under acidic conditions. This study of mutant enzymes complements insights from X-ray structures and structure−activity relationships of the wild-type enzyme for refining views of inhibitor recognition.

Scytalone dehydratase (SD,[1] EC 4.2.1.94) efficiently catalyzes the dehydrations of scytalone and vermelone, two physiological substrates within the fungal melanin biosynthetic pathway (Figure 1) (*1*−*8*). Fungal melanin, a polymer of 1,8-dihydroxynaphthalene, is used by the pathogen *Magnaporthe grisea* in forming a rigid infection structure capable of penetrating host cells (*9*, *10*). The resulting disease, known as rice blast, has significant economic impacts worldwide (*11*). The enzymes of the pathway become attractive targets for fungicide design when considering that they do not belong in plants or animals, suggesting that specific inhibitors should decrease the risk of deleterious effects occurring in off-target organisms. Early blasticides, marketed for more than 20 years, inhibit the function of 3HN reductase which catalyzes the NADPH-mediated reduction of 3HN, the product of scytalone dehydration (*12*−*14*). Whereas 3HN reductase belongs to a large family of enzymes (the short chain dehydrogenases) (*12*, *15*), SD has no known functional counterparts in plants or animals. SD is the target of newly developed blasticides (*16*−*19*), and it is the subject of a structure-based design program that has produced inhibitors with picomolar dissociation constants and with efficacious fungicidal activities (*20*−*25*).

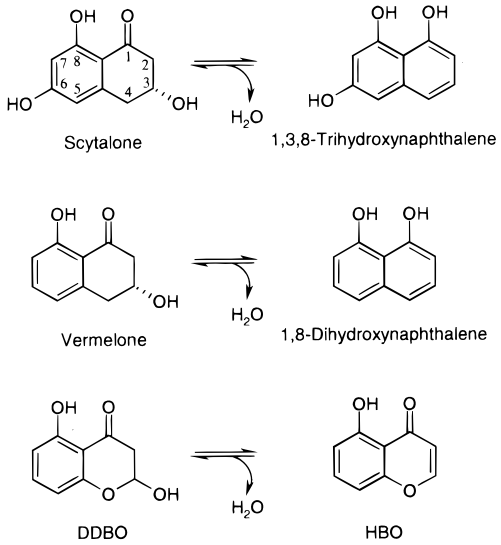

FIGURE 1: Dehydration reactions catalyzed by scytalone dehydratase.

* To whom correspondence should be addressed. Telephone: (302) 695-4280. Fax: (302) 695-4083. E-mail: doug.b.jordan@dupontpharma.com.

‡ DuPont Pharmaceuticals Company.

§ DuPont Central Research and Development.

|| DuPont Agricultural Products.

[1] Abbreviations: SD, scytalone dehydratase; DDBO, 2,3-dihydro-2,5-dihydroxy-4*H*-benzopyran-4-one; DMSO, dimethyl sulfoxide; EIMS, electrospray ionization mass spectrometry; SDS, sodium dodecyl sulfate; SDS−PAGE, SDS−polyacrylamide gel electrophoresis; 1STD, PDB accession code for the X-ray structure of scytalone dehydratase determined using crystals grown at pH 4.5; 3STD, 4STD, 5STD, 6STD, and 7STD, PDB accession codes for the X-ray structures of scytalone dehydratase determined using crystals grown at neutral pH; 3HN, 1,3,8-trihydroxynaphthalene; PCR, polymerase chain reaction; DTT, dithiothreitol; Tris, tris(hydroxymethyl)aminomethane; E1cb, elimination first-order conjugate base; SAR, structure−activity relationships.

10.1021/bi000467m CCC: $19.00
Published on Web 06/27/2000

Off and on the enzyme, scytalone undergoes E1cb-like dehydration reactions that are differentiated by the greater commitment to product formation (elimination) following enolization in the enzyme-catalyzed reaction (*6*). E1cb-like mechanisms and their relevance to enzyme-catalyzed reactions have been examined (*26*−*29*). Additionally, the enolization step of scytalone dehydration is differentiated on and off the enzyme with respect to the preference for proton abstraction from the C2 position (pro *R* preference by the enzyme and pro *S* solvolytically) (*8*, *30*). All potent inhibitors of SD maintain structural features that mimic the transient enol intermediate of the reaction coordinate for scytalone dehydration by having two strategically displayed sp2 centers in the binding pocket of the enzyme. Proof of the binding interactions involving the two sp2 centers has been delineated through X-ray structures of SD complexed with eight potent inhibitors (*20*−*24*, *31*).

Among the numerous contacts between amino acid residues and the inhibitors identified by X-ray crystallography, all but one arise from the amino acid side chain atoms rather than from backbone atoms (*20*−*24*, *31*). Clearly, this preponderance of side chain contacts offers an experimental advantage for studying many of the inhibitor interactions within the binding site, as the protein residues may be mutated to different amino acids allowing for determinations and comparisons of inhibition constants. Previously, we reported a considerable amount of information about the structure−activity relationships (SAR) of SD inhibitors (*20*−*25*), and there will be additional SAR forthcoming. Inhibitors having stepwise changes offer insights for understanding molecular recognition and become more informative when combined with X-ray crystallographic information. Having inhibitor SAR and structural information in hand, one might ask, "How can enzyme mutants offer additional value in a study of molecular recognition?" From this case study on SD, enzyme mutants corroborate some predictions and offer some unexpected results, thus refining our concepts about the factors contributing to molecular recognition.

EXPERIMENTAL PROCEDURES

Materials and General Methods. DDBO (Figure 1) was synthesized as described in ref *3*. Scytalone was purified from cultures of *rsy*$^-$ mutants of *M. grisea* (*2*). UV−vis spectrophotometric analyses were performed on HP 8452A or HP 8453 diode array spectrophotometers (Hewlett-Packard). SDS−PAGE analyses of proteins were conducted by using a PhastSystem (Pharmacia, Uppsala, Sweden). Homogeneous wild-type SD was purified as described previously (*32*). Constructions and purifications of the N131A, H110N, H110A, H85N, Y30F, Y50F, Y30F/Y50F, S129A, and S129T mutants of SD have been reported (*6*). Steady-state kinetic parameters for SD and its mutants were determined using published methods (*6*). Stoichiometries of SD mutants binding to the same potent inhibitor used previously (K_i = 9 pM) were determined as described in ref *6*. Molecular masses of SD and the mutants were determined using a Fisons VG Quattro II mass spectrometer in the electrospray ionization mode with calibration against horse heart myoglobin as an external standard. The cysteine content of the enzymes was determined colormetrically using the thiol reagent 5,5′-dithiobis(2-nitrobenzoic acid) in the presence of 0.1% SDS at pH 8.0 with anhydrous cysteine-HCl as a standard. For a table containing the molecular masses, cysteine contents, and inhibitor binding stoichiometries for the mutants prepared for this work, see the Supporting Information. ^{1}H NMR spectra were recorded on either a Varian VXR-300 NB or a Varian VXR-400-ND instrument. For details of the syntheses of inhibitors **1**−**13**, see the Supporting Information.

Preparation of Scytalone Dehydratase Mutants. Cloning and generation of recombinant plasmids were carried out using standard methods (*33*). Mutant constructs were prepared by megaprimer mutagenesis (*34*) or more standard methods. For details of the constructs for the F53A, F53L, F158L, F162L, V75A, M69A, and M69L mutants of this work, see the Supporting Information. Following sequencing, the correct mutant SD expression plasmids were transformed into *Escherichia coli* BL21(DE3) cells for protein expression. Cells containing expression vectors for F53A, F53L, F158L, F162L, V75A, M69A, M69L, or wild-type SDs were grown at 37 °C in LB medium in the presence of 100 mg/L ampicillin to between 0.5 and 0.7 OD_{600}. Induction was achieved with 1 mM isopropyl thio-β-D-galactopyranoside, which was added 3 h before harvest. These SDs were produced predominately in the soluble fraction. Purification of the mutant SDs was achieved by hydrophobic interaction chromatography followed by anion exchange chromatography essentially as described for wild-type SD (*32*).

Determination of Inhibition Constants. In method A, assay mixtures (1 mL) included 100 mM sodium phosphate, 0.2−1.0 mM DBBO (the latter concentration, approximately 67-fold larger than the K_m for the substrate for wild-type SD), 0.5% DMSO, and 0.6 nM wild-type SD at pH 7.0 and 25 °C. Reactions (10−60 s) were initiated with SD and monitored continuously at 320 nm by using an HP 8542A spectrophotometer (Hewlett-Packard). Initial rates were determined from the instrument's software fittings to a line, which is valid since the traces were linear. Competitive inhibition was found for the wild-type enzyme for the inhibitors that are described; also, the inhibitors described have counterparts that are found to bind in the scytalone binding pocket as determined from X-ray crystallographic studies (*6*, *20*−*24*). Most K_i values were determined by fitting the data to eq 1 describing competitive inhibition:

$$v = \frac{VS}{S + K_m(1 + I/K_i)} \quad (1)$$

where v is the observed velocity, V is the maximum velocity, S is the DDBO concentration, I is the inhibitor concentration, K_m is the Michaelis constant for DDBO (K_m = 15 μM for the wild-type enzyme, K_m values for the mutant enzymes are reported in ref *6* and in this work), and K_i is the dissociation constant for the inhibitor from the SD−inhibitor binary complex. Method A was used for the more catalytically active mutant enzymes where the ratio of enzyme concentration to inhibitor concentration in the incubation did not exceed 0.2.

In method B, when inhibitor concentrations in the assays were less than 4-fold in excess of the enzyme concentration (as for some inhibitors with respect to the Y50F and Y30F/Y50F mutants), K_i values were estimated with eq 2 which includes an enzyme concentration term (E) in the calculation; the other terms are as described for eq 1.

$$v = (VS)/(1 + [I - \{K_i(1 + S/K_m) + E + I - \sqrt{[K_i(1 + K/K_m) + E + I]^2 - 4IE}\}/2]/K_i(1 + S/K_m)) \quad (2)$$

The use of eq 2 instead of eq 1 lowered the determined K_i values by no more than a factor of 3.

In method C, in the case of the H85N mutant, which is so severely impaired with respect to catalysis that it would be impossible to obtain accurate K_i values by using the procedures described above, a double-equilibrium type of analysis was employed (*35*). In this method, the catalytic activity of the wild-type SD was used as the reporter of the unliganded inhibitor concentration in an incubation that included 1 mM DDBO, an inhibitor concentration affording approximately 80% inhibition of the wild-type SD under these conditions, and varying concentrations of the mutant enzyme. In the incubation, binding of the inhibitor by the mutant enzyme lowers the concentration of free inhibitor available for inhibiting the catalytic activity of the wild-type enzyme, and as a result, the rates of DDBO dehydration by wild-type SD increase as the concentration of the mutant enzyme is raised. Data from the double-equilibrium method were fitted to eq 3

$$v = (V_o)/(1 + [I - \{K_i(1 + S/K_m) + E + I - \sqrt{[K_i(1 + S/K_m) + E_m + I]^2 - 4IE_m}\}/2]/IC_{50}) + v_m \quad (3)$$

where v is the velocity of DDBO dehydration, V_o is the rate of the wild-type enzyme in the absence of inhibitor, K_i is the dissociation constant for dissociation of the inhibitor from the mutant enzyme, E_m is the concentration of the mutant enzyme (enzyme active sites) in the incubation, I is the total inhibitor concentration, IC_{50} is the concentration of inhibitor affording 50% inhibition of the wild-type SD under these conditions, S is the DDBO concentration, and v_m is the dehydration rate of the mutant enzyme under these conditions. For the H85N mutant, the values for v_m were zero. The K_m value (Michaelis constant for DDBO) for H85N is 5.7 μM (*6*).

Nonlinear least-squares fittings to eqs 1−3 were achieved with the computer program RS1 (BBN Research Systems, Cambridge, MA). All protomer enzyme concentrations (for example, E and E_m in eqs 2 and 3) were determined by using extinction coefficients at 280 nm for the proteins which were calculated by using the Peptidesort computer program within the Wisconsin Sequence Analysis Package (*36*). The calculated ϵ_{280} values are 48 850 M^{-1} cm^{-1} for the wild-type, K73A, K73Q, D31N, H85N, H110A, H110N, S129A, S129T, F53A, F53L, F158L, F162L, M69A, M69L, and V75A SDs discussed in this work. A value of 47 570 M^{-1} cm^{-1} was used for the Y30F and Y50F mutants, and 46 290 M^{-1} cm^{-1} for the Y30F/Y50F double mutant.

RESULTS

Site-Directed Mutagenesis and Analysis of Mutant Constructs. The mutant cDNAs were completely sequenced to confirm the fidelity of the PCR. All expressed mutant proteins were purified to homogeneity as judged by SDS−PAGE. EIMS indicated that the mutant proteins had the correct molecular weights (Supporting Information). Cysteine content (one per protomer) is another indication of protein purity because there is only one cysteine per enzyme protomer (Supporting Information). Active site titrations with the same potent inhibitor used previously [$K_i = 9.0 \pm 0.7$ pM for wild-type SD (*6*)] were used as an indicator of the fraction of properly folded recombinant protein (Supporting Information). Most SD enzymes reported here and before have nearly a 1:1 stoichiometry on binding the inhibitor. Variations from 1:1 stoichiometry with the inhibitor with respect to SD protomer were used to adjust the reported steady-state kinetic parameters for SD mutants F53A, F53L, and F162L, which had inhibitor:enzyme protomer stoichiometries of of 0.82, 0.88, and 0.71, respectively.

Table 1: Steady-State Kinetic Parameters for Scytalone Dehydratase and Mutants with Substrate DDBO at pH 7.0 and 25 °C[a]

enzyme	k_{cat}(DDBO) (s^{-1})	k_{cat}/K_m(DDBO) (μM^{-1} s^{-1})	K_m(DDBO) (μM)
wild-type[b]	400 ± 9	27 ± 2	15 ± 1
F53A[c]	110 ± 4	1.1 ± 0.04	100 ± 8
F53L[c]	120 ± 9	27 ± 8	4.5 ± 2
F158L	280 ± 20	4.5 ± 0.3	63 ± 8
F162L[c]	46 ± 3	0.74 ± 0.05	61 ± 8
M69A	150 ± 30	3.5 ± 0.2	41 ± 3
M69L	540 ± 30	22 ± 3	25 ± 5
V75A	21 ± 0.5	1.1 ± 0.06	20 ± 2

[a] Standard errors are indicated with the values. [b] Means and standard deviations for eight determinations. [c] Corrected for active site content (F53A, F53L, and F162L have inhibitor:enzyme protomer stoichiometries of 0.82, 0.88, and 0.71, respectively).

Steady-State Kinetic Parameters. Steady-state kinetic constants for the SD-catalyzed dehydration of the synthetic substrate DDBO are listed in Table 1 for the wild-type and mutant SD enzymes prepared for this work. The mutations of the active site hydrophobic residues cause a ≤36-fold decrease in k_{cat}/K_m and a 20-fold decrease in k_{cat}, effects considerably smaller than those seen with most of the mutations of the hydrophilic residues studied previously (*6*).

Inhibitor Binding Constants in the Mutated Hydrophilic Binding Site of the Enzyme. Inhibitor binding constants for the wild-type SD and several mutant enzymes are listed in Table 2 for inhibitors having a common phenylpropyl linkage to seven different hydrophilic groups that lie in the hydrophilic region of the binding site (Figure 2). The *N*-phenylpropyl substituent was selected because it extends into the hydrophobic region of the binding pocket and produces inhibitors with affinities lower than those of the better optimized substituents. This allows for direct determination of binding potencies for the mutant enzymes that are catalytically impaired. K_i values are raised for the wild-type SD by factors of 100−1000 in comparison to more optimized hydrophobic substituents (compare with analogues in Table 3). Even though the inhibitors of Table 2 are less potent than the optimized examples, it was necessary to correct for the enzyme concentration in calculating the K_i values for the Y50 and Y30F/Y50F mutant enzymes by using eq 2 (method B). In the case of H85N, whose k_{cat} is 10^5-fold lower than that of wild-type SD, it was necessary to use the catalytic activity of the wild-type SD as a reporter of inhibitor binding to the mutant protein (method C). The mutations produce large differences in binding affinities ranging from 10-fold enhancements to 1100-fold reductions.

Table 2: K_i Values (nanomolar) for Scytalone Dehydratase Mutants at pH 7.0 and 25 °C[a]

enzyme	1	2	3	4	5	6	7
wild-type	12 ± 0.5	2.2 ± 0.2	13 ± 0.7	3.8 ± 0.2	3.6 ± 0.4	15 ± 2	4.6 ± 0.2
N131A	130 ± 1	37 ± 1	1900 ± 100	540 ± 40	4100 ± 300	1100 ± 50	42 ± 2
H110N	240 ± 10	81 ± 2	96 ± 0.5	36 ± 1	710 ± 50	150 ± 10	15 ± 2
H110A	360 ± 25	130 ± 7	400 ± 40	51 ± 3	900 ± 20	ND[b]	ND[b]
H85N[c]	89 ± 6	29 ± 2	210 ± 50	200 ± 20	120 ± 20	20 ± 1	3.3 ± 0.2
Y30F	3.3 ± 0.2	1.9 ± 0.09	80 ± 5	2.6 ± 0.05	2.4 ± 0.07	33 ± 1	3.1 ± 0.2
Y50F[d]	1.2 ± 0.1	0.35 ± 0.05	10 ± 1	0.70 ± 0.2	1.0 ± 0.2	3.2 ± 0.08	4.0 ± 0.6
Y30F/Y50F[d]	36 ± 3	34 ± 0.5	150 ± 4	11 ± 1	6.4 ± 1	ND[b]	ND[b]
S129A	19 ± 2	3.0 ± 0.1	16 ± 1	4.9 ± 0.2	6.8 ± 0.7	25 ± 0.6	4.3 ± 0.2
S129T	2.6 ± 0.09	0.66 ± 0.04	150 ± 10	26 ± 0.1	81 ± 8	230 ± 30	42 ± 2
F53A	930 ± 110	450 ± 6	320 ± 20	97 ± 7	70 ± 9	ND[b]	ND[b]
F53L	39 ± 0.5	17 ± 0.6	12 ± 1	2.5 ± 0.3	52 ± 1	ND[b]	ND[b]
F158L	110 ± 6	36 ± 1	120 ± 5	19 ± 0.1	ND[b]	ND[b]	ND[b]
F162L	86 ± 0.1	33 ± 1	100 ± 0.1	18 ± 1	ND[b]	ND[b]	ND[b]
V75A	5.1 ± 0.1	1.1 ± 0.06	19 ± 0.8	1.9 ± 0.2	ND[b]	14 ± 0.7	0.59 ± 0.01
K73A	19 ± 0.7	3.0 ± 0.1	20 ± 0.8	4.7 ± 0.3	ND[b]	ND[b]	ND[b]

[a] Standard errors from the determinations are indicated with the values. Unless indicated otherwise, method A was employed in the determinations. [b] ND, not determined. [c] Determined by method C. [d] Determined by method B.

Table 3: K_i Values (picomolar) for Scytalone Dehydratase Mutants at pH 7.0 and 25 °C[a]

enzyme	8	9	10	11	12	13
wild-type	11 ± 1	25 ± 2	20 ± 1	18 ± 0.5	80 ± 5	580 ± 40
F53L	ND[b]	76 ± 8	280 ± 30	84 ± 6	860 ± 100	2500 ± 300
F158L	ND[b]	140 ± 10	590 ± 80	290 ± 20	1500 ± 100	5400 ± 300
F162L	ND[b]	280 ± 50	900 ± 70	670 ± 50	3900 ± 60	12000 ± 1000
M69L	14 ± 0.7	20 ± 2	48 ± 4	870 ± 40	1700 ± 200	6600 ± 600
V75A	ND[b]	250 ± 20	1100 ± 20	1300 ± 90	3800 ± 400	12000 ± 800

[a] Standard errors from the determinations using method A are indicated with the values. [b] ND, not determined.

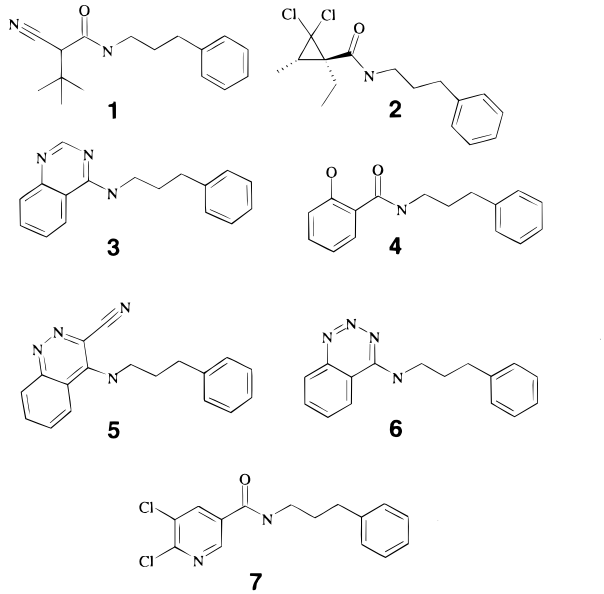

FIGURE 2: Inhibitors that display variations in the hydrophilic region of the SD binding site.

Inhibitor Binding Constants in the Mutated Hydrophobic Site of the Enzyme. As the mutations of the hydrophobic residues have catalytic activities approximating that of wild-type SD, considerably more potent enzyme inhibitors could be examined. The inhibitors have a common cyanoacetamide group linked to varied hydrophobic groups (Figure 3). K_i values were determined by using the more simple eq 1 which does not include an enzyme concentration term as the inhibitor concentrations were at least 5 times greater than the concentration of the respective enzymes in the incubations. Mutations F53L, F158L, F162L, M69L, and V75A

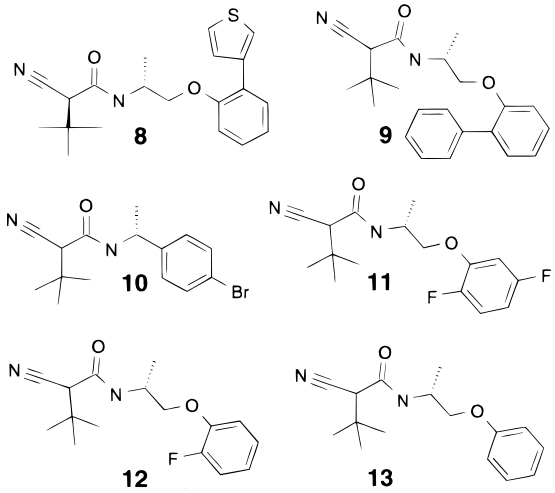

FIGURE 3: Inhibitors that display variations in the hydrophobic region of the SD binding site.

produce K_i values that range from 3- to 70-fold larger than that of wild-type SD (Table 3). K_i values, determined for some of the mutated hydrophobic side chains against the inhibitors having varied hydrophilic groups, increase by as much as 200-fold in comparison to the wild-type values (Table 2).

DISCUSSION

Here we examine through site-directed mutagenesis the binding interactions of the side chains of the 11 amino acid residues thought to interact most closely with 13 inhibitors from analyses of several reported X-ray structures: 1STD (*21*, *31*), 3STD (*20*), 4STD (*21*), 5STD (*21*), 6STD (*21*), and 7STD (*21*). The SD binding pocket may be divided into

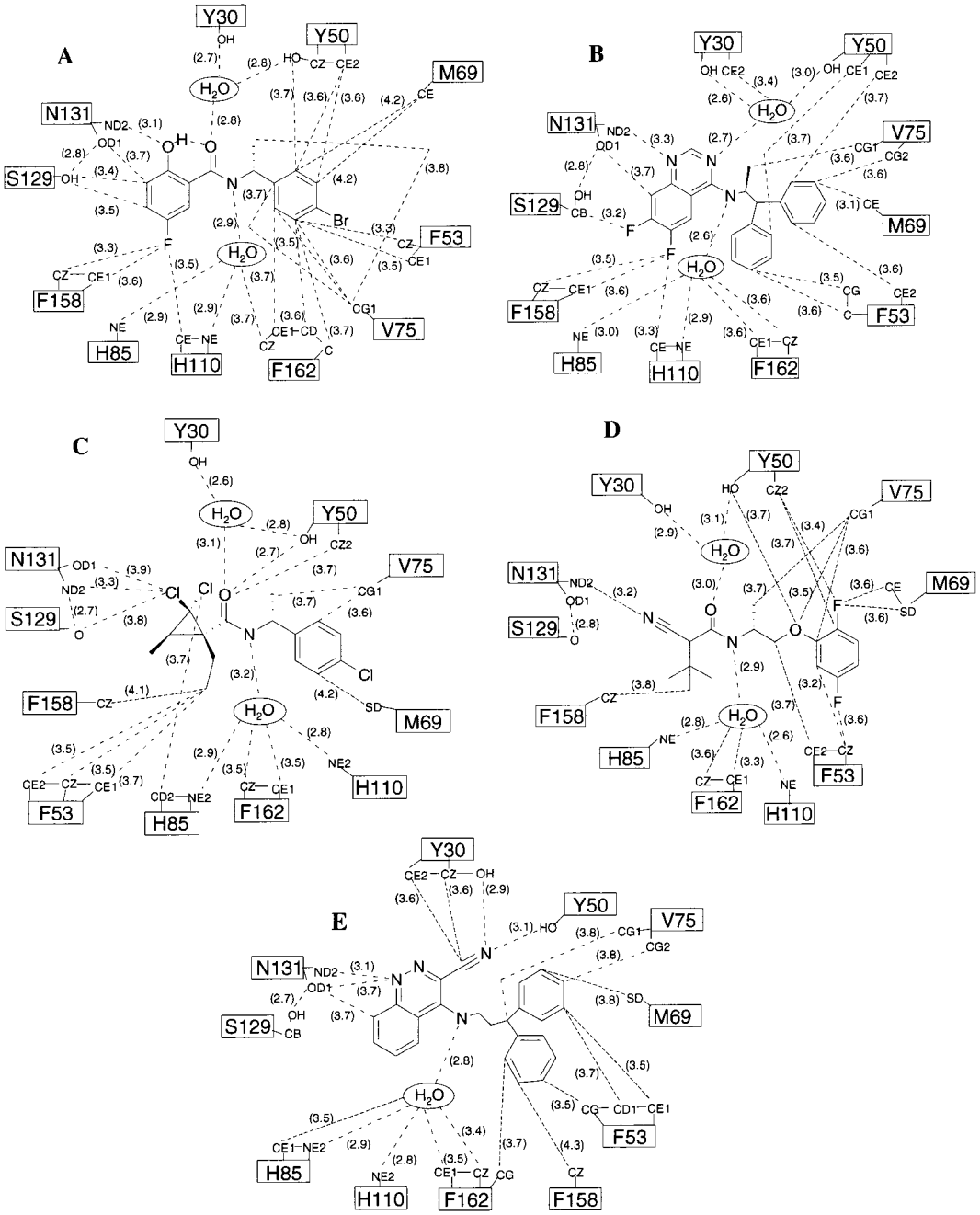

FIGURE 4: Binding contacts of five inhibitors with the 11 side chains of SD examined in this study as determined by X-ray crystallography: (A) a salicylamide (*18*), (B) an aminoquinazoline (*18*), (C) a cyclopropane carboxamide (*18*), (D) a cyanoacetamide (*19*), and (E) a cyanocinnoline (*17*). Distances are in angstroms.

two portions, a hydrophilic region containing the catalytic center of SD that includes the side chains of residues N131, S129, H85, H110, Y30, and Y50 and two crystallographic water molecules and a hydrophobic region that includes the side chains of residues F53, F158, F162, M69, and V75.

Figure 4A−E depicts in detail the binding interactions of five inhibitors with the side chains of the 11 residues examined in this study as determined by X-ray analysis. The salicylamide in panel A is positioned to have hydrogen bonding interactions with N131, Y30, and Y50, the latter two interactions being indirect through a crystallographic water molecule. What is the contribution of the hydrogen bonds to inhibitor binding potency? Here we obtain a measure of the strength of the interactions by mutations of Y30 and Y50 to phenylalanines, individually and in a double mutant, and by mutation of N131 to an alanine. H85 and H110 are bonded to a second crystallographic water molecule that accepts a hydrogen from the NH group of the inhibitor. The influence of the imidazoles on inhibitor binding is characterized by mutations of H85 to an asparagine and H110 to both an asparagine and an alanine. In all of the SD structures that are studied, S129 forms a hydrogen bond with N131, which could add rigidity to this portion of the binding pocket. Though there are no direct hydrogen bonding interactions between S129 and any of the inhibitors as determined by X-ray analysis, when substrate scytalone is docked in place of the inhibitor, the C6 hydroxyl group of scytalone donates a hydrogen to the S129 hydroxyl oxygen (*8*). Here we examine the effects on binding of mutations of S129 to alanine and threonine. Panel B details the interactions

with an aminoquinazoline inhibitor of SD. Clearly, the hydrogen bonding contacts shared with N131, tyrosines 30 and 50 (through a water molecule), and histidines 85 and 110 (through a water molecule) resemble those described above for the salicylamide. This mimicry was the result of a design program achieved before the availability of X-ray crystallographic information for SD (*37*). It is expected that the hydrogen bonding and strength of binding of the inhibitors in panels A and B of Figure 4 will be disrupted by mutations of the hydrophilic residues in similar fashions. Like the inhibitors in panels A, B, and E of Figure 4, those in panels C and D should retain the hydrogen bonding network comprising histidines 85 and 110 and tyrosines 30 and 50 through the two crystallographic water molecules, whereas they should not have hydrogen bonding interactions with N131. The inhibitor in panel E is a cyanocinnoline, whose cyano group displaces the water molecule that bridges the hydroxyl groups of Y30 and Y50 with other inhibitors (*20*). Chen et al. (*20*) speculated that the direct contacts between the cyano group and the hydroxyl groups of the two tyrosine residues provide enough of a binding enhancement to overcome the loss of the favorable enthalpic contribution associated with binding of the water molecule. These and other interactions of the hydrophilic residues are tested by examining the effects of mutations on binding affinities for the inhibitors shown in Figure 2, which contain varied hydrophilic groups connected to a common hydrophobic group.

Hydrophobic interactions between the inhibitors of Figure 4 are of considerable interest as they contribute 2−4 kcal/mol in binding energy in optimized inhibitors. Here we examine the influence of the side chains of five residues (F53, F158, F162, M69, and V75) implicated in inhibitor binding through alterations to leucines and alanines. Inhibitors contain a common hydrophilic cyanoacetamide group linked to a set of hydrophobic substituents (Figure 3).

Roles of Hydrophilic Residues. We studied inhibitor binding properties of site-directed mutants of SD hydrophilic residues that have defined roles in the catalytic cycle (*6*). In some cases, the mutations impair catalytic activity to an extent that would preclude determinations of picomolar binding constants for fully optimized inhibitors. Employing the phenylpropyl substituent as a common hydrophobic moiety (unoptimized for binding affinity so that it produces K_i values that are 100−1000-fold higher than those of optimized groups) to varied amide and amine functionalities allowed determinations of the mutation effects on the binding of the more hydrophilic groups of the inhibitors. The phenylpropyl group is well accommodated in the active site of SD according to docking studies where it occupies a space similar to that occupied by optimized side chains of the inhibitors in Figure 4 (panels A, C, and D). Having the phenylpropyl moiety in common allows for a simple comparison of inhibitor molecules, whose optimized hydrophobic portions depend on the structure of the hydrophilic portion (*23*). Mutation of K73 served as a negative control as the native residue has no role in catalysis and is not part of the substrate or inhibitor binding site (*6*). Inhibition constants for the K73A mutant were determined for several of the inhibitors that have altered hydrophilic groups; the inhibition constants proved to be similar to those of wild-type SD (Table 2). Numerous hydrophilic groups of inhibitors (including some not reported) were investigated so that the interpretations presented below could be generalized for ligand interactions with SD.

S129A and S129T. Analyses of the alanine mutant of S129 determined that the hydroxyl side chain contributes to productive binding of scytalone (which contains a hydroxyl group that can interact with the residue's side chain hydroxyl) but not to that of substrates vermelone and DDBO (Figure 1), which lack an analogous hydroxyl group for interactions with the amino acid side chain (*6*). The inhibitors examined do not display functionalities toward the serine hydroxyl, so the lack of significant effects on the K_i's determined for the alanine mutation (ratios of S129A to wild-type K_i values range from 0.9 to 1.9) is not surprising. The similar K_i values establish that the hydrogen bonding interaction between the hydroxyl of S129 and the side chain carbonyl of N131 does not significantly contribute to shaping the enzyme's active site for ligand binding.

Mutation to threonine places the side chain methyl group into a position that can affect binding. The three inhibitor classes represented by **3**−**5** with aromatic groups displayed toward S129 bind less well to S129T than to the wild type (by factors of 12, 7, and 23, respectively), while the two inhibitor classes represented by **1** and **2** bind better (by factors of 5 and 3, respectively). Modeling of the S129T mutation for each of the crystal structures obtained for the five inhibitor classes shows steric overlaps for the extra methyl group of S129T with **3**−**5** but not with **1** and **2**. Inhibitors **1** and **2** likely gain small increases in binding potency with S129T over the wild type through enhanced van der Waals contacts, while steric encumbrance is detrimental to binding potency for **3**−**5**.

H85N, H110A, and H110N. H85 and H110 indirectly contact the inhibitors of Figure 4 (and all inhibitors in other X-ray structures) with a water molecule bridging the ϵ-nitrogens of the imidazoles to the inhibitor NH through hydrogen bonds. This bridging water molecule has been described as the water of dehydration in the catalytic reaction because modeling of scytalone into the binding pocket places the leaving hydroxyl group in proximity to the position of this crystallographic water molecule (*31*). The water complexed with the H85 and H110 can be thought of as a base that accepts a hydrogen from the NH of the inhibitors in forming hydrogen bonds. The mutations of H85 and H110 decrease the binding potencies of the inhibitors by factors ranging from 1 to 250. Mutation of H110 to asparagine displays a carboxamide capable of hydrogen bonding, while the mutation to alanine does not. H110A has only marginally larger K_i's than H110N in all the cases that are examined, thus substantiating that the basicity of the imidazole side chain is the significant component of tight binding interactions. Enhanced basicity of H85 through its contact with the carboxylate of D31 is not a factor in the binding of inhibitors as judged from there being generally lower K_i's for H85N than for H110N.

Inhibitor **5** is more greatly affected by the mutations (200- and 250-fold attenuations in the potency of binding to H110N and H110A, respectively, in comparison to that of wild-type SD) than inhibitors **3** (7.4- and 31-fold attenuations) and **6** (10-fold attenuation for H110N). The cyano substituent of **5** is described below as entering into a steric encumbrance with the hydroxyls of Y30 and Y50. To the extent that this

occurs, it could shift the molecule toward H110, giving shorter and stronger hydrogen bonds, thus accounting for the attenuation of binding potencies with the H110N and H110A mutants of SD. Thus, inhibitor binding to H110 is considered to be influenced by an inhibitor functionality remote from the residue.

Y30F and Y50F. k_{cat}(DDBO) values of Y30F and Y50F are 10- and 100-fold lower than that of the wild type, respectively; the effects of the mutations are additive as the catalytic activity of the double mutant Y30F/Y50F is 1000-fold lower than that of the wild type. K_m(DDBO) values for the individual and double mutants are similar to that of the wild type (*6*). These findings were interpreted as having the water molecule relay the proton donating capability of the tyrosine hydroxyls to the single coordination site available on the substrate carbonyl in the transition state of the enolization. Similarly, it could be envisioned that the water molecule protonates the carbonyls of compounds **1**, **2**, **4**, and **7** and the 3-position nitrogen of compounds **3** and **6**, relaying the proton donating capabilities of the two tyrosines. However, neither of the individual tyrosine mutations greatly affects inhibitor binding. With the exception of the binding of **3** with the Y30F mutant, all the binding interactions of the inhibitors are slightly tighter with the tyrosine mutants than with wild-type SD. The single tyrosine mutations still allow for a hydrogen bonding network between inhibitors, a water molecule, and the remaining tyrosine. Indeed, an X-ray structure of the Y50F in complex with a salicylamide inhibitor (an analogue of **1**) shows that the associated water molecule is retained (*6*). It is reasonable that the three available hydrogen bonds among the tyrosines, the water molecule, and an inhibitor would not exist concurrently, and there is presumably a dynamic equilibrium that has the hydrogen bonding network shifting back and forth. A molecular dynamics study suggested that the water complexed with Y30, Y50, and an inhibitor is not held as tightly as the water molecule complexed with H85, H110, and an inhibitor (*38*), again indicating that the hydrogen bonding network of the former is weaker than the latter.

All of the inhibitors that we studied bind less well (by 4−20-fold) to the Y30F/Y50F double mutant (wherein two hydroxyls of the inhibitor−water hydrogen bonding network are lost) than to the wild type. The nonadditivity of the single mutations confirms that the overall hydrogen bonding network around the water molecule contributes to inhibitor binding. The relief of steric congestion around the water molecule may mask the effect of losing a transient hydrogen bond in the single Y to F mutations. The double mutation reflects the effect of losing a full hydrogen bond outright with the inhibitors. Whereas each tyrosine hydroxyl is individually important for stabilizing the transition state during catalysis, each is individually less important to the ground-state situation of inhibitor binding. Thus, the inhibitor interactions with Y30 and Y50 may be considered as ground-state interactions instead of mimicking the transition state of the enolization.

The nitrile of inhibitor **5** was incorporated to displace the water molecule associated with the two tyrosine residues, and the 4-fold increase in SD binding potency relative to that of **3** can be attributed to doing so as designed (*20*). An X-ray structure of an analogue of **5** (Figure 4E) shows that the nitrile displacing the water molecule forms contacts with the hydroxyl groups of Y30 and Y50 (*21*). However, the contacts of the tyrosine hydroxyls are not favorable as reflected in the data of this work; **5** binds to Y30F and Y50F 1.5- and 2.6-fold, respectively, more tightly than to the wild type. Hence, the favorable binding engendered by the nitrile of **5** to wild-type SD is due to interactions of other side chains (mainly N131 and H110) with inhibitor atoms remote from the nitrile.

N131A. The inhibitors studied display varying functionalities toward N131 as determined by X-ray crystallography. The first crystal structure determined for SD complexed with a salicylamide inhibitor analogous to **4** (Figure 4A) has the phenol oxygen positioned 3.1 Å from the N131 side chain NH_2 forming a hydrogen bond. The extent of binding of **4** is diminished 140-fold by the N131A mutation, and this hydrogen bond with N131 amounts to the most important single interaction between the enzyme and the inhibitor among the mutants. This hydrogen bond is also important to the recognition of the enzyme's substrates, which similarly contain a phenolic oxygen (*6*). The design of the salicylamide class of inhibitors was based, in part, on the structural resemblance to the substrate and its transition state for conversion to product (*21*).

The 1-position nitrogen atoms of the amino heterocycles **3**, **5**, and **6** are also poised to accept a hydrogen from N131, and the mutation to alanine also causes the greatest deterioration in binding potency that we observed among the mutants. Replacement of the 1-postion nitrogen in analogues of **3**, **5**, or **6** with a carbon atom damages inhibitory potency to wild-type SD considerably, further underscoring the importance of the hydrogen bond with N131 to binding (*20*). The deterioration in binding potency for N131A with **5** is considerably greater (1100-fold) than with **3** and **6** (140- and 73-fold, respectively). The nitrile of **5** lies far away from N131 and is adjacent to the hydroxyls of Y30 and Y50 whose mutation to phenylalanine increases the binding potency (see above). The steric encumbrance created by the nitrile with the tyrosine hydroxyls can be envisioned to push the entire inhibitor molecule **5** toward N131, creating a hydrogen bond that is shorter than that existing with **3** and **6** and accounting for the greater influence of the asparagine carboxamide on the binding of **5**.

Cyclopropane **2** displays its dichloromethylene toward N131 such that the two chlorine atoms are nearly coplanar with the three heavy atoms of the side chain carboxamide as determined from the X-ray structure of a close-in analogue bound to SD (Figure 4C) (*21*). Since chlorine is not a good hydrogen acceptor, the N131A mutation is not as deleterious to binding as for inhibitors **3**−**6**. One of the chlorine atoms of **2** could be considered to form a good electrostatic interaction with the NH_2 of the N131 side chain carboxamide, while the other would form a poor one with the carboxamide carbonyl.

The nitrile of **1** is directed toward N131 as determined from the X-ray structure of the close-in analogue shown in Figure 4D (*22*). Nitriles are poor hydrogen acceptors in forming hydrogen bonds and have a strict geometrical requirement due to the sp hybridization of the electron lone pair. Correspondingly, the N131A mutation decreases the extent of binding of **1** by 11-fold, much less than the effect seen with the better hydrogen accepting inhibitors **3**−**6**. Modeling of inhibitor **7** in the SD binding pocket has a

chlorine atom displayed toward the carboxamide of N131, and there is modest decrease in binding potency (9-fold) realized by the N131A mutation.

Roles of Hydrophobic Residues in Catalysis. The hydrophobic residues chosen for mutational analysis form a barrel around the center of the oblong SD active site. The model of scytalone in the active site has these residues (with the exception of M69) encircling the substrate off-center to the saturated ring. The mutations of the hydrophobic residues debilitate SD catalysis to a smaller extent than most of the mutations in the hydrophilic residues, because they are not directly involved in the bond-breaking and -forming events of the transition state. However, the structural integrity in the hydrophobic environment of the active site would be expected to be disrupted by mutations either to less hydrophobic residues or to structurally distinct ones (e.g., of aromatic residues to aliphatic residues). Correspondingly, the F53A mutant has a k_{cat}/K_m nearly 25-fold smaller than that of wild-type SD. This effect is due a 7-fold increase in K_m and a 3-fold decrease in k_{cat}, indicating there is a deterioration in both substrate binding and catalysis. This is certainly reasonable as phenylalanine could facilitate catalysis more than alanine by providing shape recognition for substrate binding and by providing a lipophilic environment for transient stabilization of the product before its release to solvent.

The mutations of phenylalanine to leucine vary in effect from nearly no debilitation in k_{cat}/K_m for F53L to a 6-fold debilitation for F158L and a 36-fold debilitation for F162L. In the case of F53L, a 3-fold decrease in k_{cat} compensates for a 3-fold reduction in K_m, the large lipophilic leucine side chain serving well as a surrogate for phenylalanine. F162 is of note since it lines the binding pocket of the histidine-associated water molecule (and by inference the leaving hydroxyl of substrate) of the active site by the edge of its aromatic ring. This contrasts with the interactions of the remaining hydrophobic residues investigated in that there is a hydrophilic−hydrophobic interaction indicated rather than hydrophobic−hydrophobic interactions. The edge orientation of the F162 aromatic ring could display hydrogen atoms for a favorable electrostatic interaction with the substrate hydroxyl (product water molecule). The V75A and M69A mutations also debilitate k_{cat}/K_m significantly (25- and 8-fold, respectively), though they are less closely associated with substrate. It is clear that the native hydrophobic residues enhance catalysis though they do not directly mediate bond-forming or -breaking steps of the SD-catalyzed reaction.

Roles of Hydrophobic Residues in Inhibitor Binding. Hydrophobic interactions between the inhibitor and enzyme can be a complex interplay of steric repulsion, conformational flexibility, and desolvation energies along with weak van der Waals and electrostatic forces (*39*). We anticipated that the correlation seen from the binding of inhibitors to SD mutants might start to sort out some of these interrelated interactions.

Phenylalaine Mutations. The K_i's of all the inhibitors studied increase with the three phenylalanine to leucine mutations (F53L, F158L, and F162L) for inhibitors having varied hydrophobic portions (Table 3); hence, the structural integrity and hydrophobic nature of the binding pocket are compromised by the mutations. Increases in K_i values range from 3- to nearly 50-fold, with F162L affording consistently the greatest drop in binding potency. F162 does not contact the inhibitors directly but rather borders the NH-bound water molecule that is important to inhibitor binding potency. Therefore, F162 gives some definition to the binding pocket around the water molecule that is compromised by its mutation to leucine.

The mutant binding data support the true orientation of F158 in lining the active site. All of the more recent SD crystal structures (3STD, 4STD, 5STD, 6STD, 7STD, and others) have been determined using crystals grown at neutral pH and have the side chain of F158 abutting the inhibitors. However, the original SD X-ray structure (1STD) was determined from crystals grown at pH 4.5 and resulted in a conformational change between residues 154 and 160 that oriented the side chain of F158 away from the inhibitor binding site into the solvent (*21*, *31*). Since the SD kinetic assays and inhibitor binding studies are carried out at pH 7.0 where the enzyme is stable and catalytic activity is maximal, it fits that the F158L mutation would affect binding of the studied inhibitors.

M69L and V75A. The crystal structure of SD in complex with **11** (*22*) shows that the side chain terminal methyl group and the sulfur atom of M69 border the 2-F atom of the phenoxy group and that the CG1 methyl group of Val75 lines the binding pocket facing the π-cloud of the phenoxy group (Figure 4D). Thus, the two residues offer a hydrophobic and electrostatic reciprocal to the lipophilic and electronegative aromatic ring in the fluorine atom region. The progression in going from the unsubstituted phenoxy group in **13** to the 2-F substituted phenoxy group of **12** and the 2,5-diF-phenoxy group of **11** increases binding potency to wild-type SD by 7- and 4-fold, respectively. The same inhibitor progression increases binding potency for the two mutant enzymes to a similar extent, indicating that the enhancements in binding potency to the wild-type SD with the addition of fluorine atoms are mainly attributable to the more favorable desolvation energies intrinsic to the more lipophilic inhibitors.

The CG1 carbon of V75 also offers a measure of recognition for the methyl group at the chiral N-substituent of the inhibitors. The distances between the CG1 atom and the methyl groups of the compounds in Figure 4 are 3.7−3.8 Å as seen in the respective crystal structures with SD. Mutating the valine to alanine raises the K_i of those compounds containing an analogous methyl group (compounds **9**−**13**) by 10−70-fold. In contrast, compounds without the methyl group (**1**−**4**, **6**, and **7**) are less affected by the mutation, and some bind more strongly to the V75A mutant than to wild-type SD.

In the analogue series **8**−**13**, large 2-position substituents such as the thiophene and phenyl of **8** and **9** lower the K_i with wild-type SD. Whereas the K_i becomes larger for M69L with **11**−**13**, which have small 2-substituents, it is nearly unaffected with **8** and **9**. We speculate that the large substituents displace the M69 side chain (and the leucine side chain of the M69L mutant) outward toward solvent, inducing a larger binding cavity. The detrimental effect of the M69 side chain displacement is counterbalanced by accommodation of the phenyl or thiophene substituents into the resultant hydrophobic environment. From the crystal structure of the SD complex with **11**, Y50 would also have to move to accommodate bulkier substituents. A preliminary crystal structure of **9** complexed with SD corroborates that

the side chain of M69 is rotated toward the solvent with the 2-position phenyl group of **9** occupying the vacated space (Z. Wawrzak, personal communication).

CONCLUSIONS

Analyses of inhibitor interactions with the SD mutants provide information leading to significant enhancements in our understanding of the enzyme that may not be gleaned from X-ray structures of SD−inhibitor complexes and from SAR of inhibitors with the wild-type SD. The information gives a measure of the strength of binding interactions. Now we know that the hydrogen bond between the hydroxyl group of S129 and the carboxamide of N131 (always present in X-ray structures) is unimportant in shaping the active site. The individual hydroxyl groups of Y30 and Y50 (which appear to interact with all inhibitors) do not contribute to inhibitor binding even in the case where the inhibitor displays a cyano group toward them. The two tyrosine hydroxyl groups interact with sp2 centers of the inhibitors (through a crystallographic water) that are analogous to the sp2 center of the substrate. The hydrogen bonding network encompassing the basic side chains of H85 and H110 with a second crystallographic water molecule provides considerable strength to inhibitor binding, consistent with the second sp2 center of the inhibitors (not present in the substrate) mimicking a transient intermediate in the enolization of substrate. H85, H110, and N131 interactions with inhibitors are influenced strongly by inhibitor atoms that are remote from the side chains of the residues. The carboxamide of N131 donates a hydrogen in forming a strong hydrogen bonding interaction with inhibitors that display a good hydrogen acceptor. The side chain of V75 is a recognition element for the chiral methyl group contained in some inhibitors. The side chain of F158 has significant interactions with inhibitors which is consistent with the residue being displayed toward the inhibitor as seen in X-ray structures that used crystals grown at neutral pH; it is inconsistent with the X-ray structures that used crystals grown under acidic conditions where the side chain is displayed toward solvent. F162 has significant influences on inhibitor binding even though there are no direct contacts of the residue's side chain with inhibitors; its role is likely to constrain the crystallographic water and ensure a strong hydrogen bonding network.

ACKNOWLEDGMENT

We thank Ya-Jun Zheng for helpful discussions. We thank John Bisaha, Robert Pasteris, and Simon Xu for their contributions to the synthesis of inhibitors.

SUPPORTING INFORMATION AVAILABLE

Synthesis of inhibitors **1**−**13** (Figures 2 and 3), the constructs of SD site-directed mutants (F53A, F53L, F158L, F162L, V75A, M69A, and M69L), and a table describing the electrospray mass spectroscopic analyses, cysteine determinations, and inhibitor binding stoichiometries for the mutants prepared for this work are presented (12 pages). This material is available free of charge via the Internet at http://pubs.acs.org.

REFERENCES

1. Bell, A. A., and Wheeler, M. H. (1986) *Annu. Rev. Phytopath. 24*, 411−451.
2. Chumley, F. G., and Valent, B. (1990) *Mol. Plant-Microbe Interact. 3*, 135−143.
3. Thompson, J. E., Basarab, G. S., Pierce, J., Hodge, C. N., and Jordan, D. B. (1998) *Anal. Biochem. 256*, 1−6.
4. Thompson, J. E., and Jordan, D. B. (1998) *Anal. Biochem. 256*, 7−13.
5. Jordan, D. B., Basarab, G. S., Steffens, J. J., Lundqvist, T., Pfrogner, B. R., Schwartz, R. S., and Wawrzak, Z. (1999) *Pestic. Sci. 55*, 277−280.
6. Basarab, G. S., Steffens, J. J., Wawrzak, Z., Schwartz, R. S., Lundqvist, T., and Jordan, D. B. (1999) *Biochemistry 38*, 6012−6024.
7. Steffens, J. J., Basarab, G. S., Schwartz, R. S., Lundqvist, T., Wawrzak, Z., and Jordan, D. B. (1999) in *Modern Fungicides and Antifungal Compounds II* (Lyr, H., Russell, P. E., Dehne, H.-W., and Sisler, H. D., Eds.) pp 121−130, Intercept Ltd., Andover, Hampshire, U.K.
8. Jordan, D. B., Zheng, Y.-J., Locket, B. A., and Basarab, G. S. (2000) *Biochemistry 39*, 2276−2282.
9. Howard, R. J., and Ferrari, M. A. (1989) *Exp. Mycol. 13*, 403−418.
10. Howard, R. J., and Valent, B. (1996) *Annu. Rev. Microbiol. 50*, 491−512.
11. Ou, S. H. (1985) in *Rice Diseases*, 2nd ed., pp 109−201, C. A. B. International, Slough, U.K.
12. Andersson, A., Jordan, D. B., Schneider, G., and Lindqvist, Y. (1996) *Structure (London) 4*, 1161−1170.
13. Thompson, J. E., Basarab, G. S., Andersson, A., Lindqvist, Y., and Jordan, D. B. (1997) *Biochemistry 36*, 1852−1860.
14. Liao, D.-I., Basarab, G. S., Gatenby, A. A., and Jordan, D. B. (2000) *Bioorg. Med. Chem. Lett. 10*, 491−494.
15. Jornvall, H., Persson, B., Krook, M., Atrian, S., Gonzalez-Duarte, R., Jeffrey, J., and Ghosh, D. (1995) *Biochemistry 34*, 6003−6013.
16. Kurahashi, Y., Sakawa, S., Kinbara, T., Tanaka, K., and Kagabu, S. (1997) *Nippon Noyaku Gakkaishi 22*, 108−112.
17. Tsuji, G., Takeda, T., Furusawa, I., Horino, O., and Kubo, Y. (1997) *Pestic. Biochem. Physiol., 57*, 211−219.
18. *Agrow* (1997) Vol. 287, pp 21−22, PJP Publications Ltd.
19. Sieverding, E., Hirooka, T., Nishiguchi, T., Yamamoto, Y., Spadafora, V. J., and Hasui, H. (1998) in *Proceedings of the 1998 Brighton Conference—Pests and Diseases*, Vol. 2, pp 359−366, British Crop Protection Council, Brighton, England.
20. Chen, J. M., Xu, S. L., Wawrzak, Z., Basarab, G. S., and Jordan, D. B. (1998) *Biochemistry 37*, 17735−17744.
21. Wawrzak, Z., Sandalova, T., Steffens, J. J., Basarab, G. S., Lundqvist, T., Lindqvist, Y., and Jordan, D. B. (1999) *Proteins: Struct., Funct., Genet. 35*, 425−439.
22. Jordan, D. B., Lessen, T., Wawrzak, Z., Bisaha, J. J., Gehret, T. C., Hansen, S. L., Schwartz, R. S., and Basarab, G. S. (1999) *Bioorg. Med. Chem. Lett. 9*, 1607−1612.
23. Basarab, G. S., Jordan, D. B., Gehret, T. C., Schwartz, R. S., and Wawrzak, Z. (1999) *Bioorg. Med. Chem. Lett. 9*, 1613−1618.
24. Jennings, L. D., Wawrzak, Z., Amorose, D., Schwartz, R. S., and Jordan, D. B. (1999) *Bioorg. Med. Chem. Lett. 9*, 2509−2514.
25. Jennings, L. D., Rayner, D. R., Jordan, D. B., Okonya, J., Basarab, G. S., Amorose, D. K., Anacelerio, B. M., Gehret, T. C., Lee, J. K., Schwartz, R. S., and Whitmore, K. A. (2000) *Bioorg. Med. Chem. 8*, 897−907.
26. Gerlt, J. A., Kozarich, J. W., Kenyon, G. L., and Gassman, P. G. (1991) *J. Am. Chem. Soc. 113*, 9667−9669.
27. Gerlt, J. A., and Gassman, P. G. (1992) *J. Am. Chem. Soc. 114*, 5928−5934.
28. Gerlt, J. A., and Gassman, P. G. (1993) *Biochemistry 32*, 11943−11952.
29. Anderson, V. E. (1998) in *Comprehensive Biological Catalysts*, Vol. 2, pp 115−133, Academic Press, New York.
30. Basarab, G. S., Jordan, D. B., and Zheng, Y.-J. (2000) *Org. Lett. 2*, 1541−1544.

31. Lundqvist, T., Rice, J., Hodge, C. N., Basarab, G. S., Pierce, J., and Lindqvist, Y. (1994) *Structure (London) 2*, 937−944.
32. Lundqivst, T., Weber, P. C., Hodge, C. N., Braswell, E. H., Rice, J., and Pierce, J. (1993) *J. Mol. Biol. 232*, 999−1002.
33. Sambrook, J., Fritsch, E. F., and Maniatis, T. (1989) *Molecular Cloning. A Laboratory Manual*, 2nd ed., Cold Spring Harbor Laboratory Press, Cold Spring Harbor, NY.
34. Aiyar, A., and Leis, J. (1993) *BioTechniques 14*, 366−368.
35. Basarab, G. S., and Jordan, D. B. (1999) *Biochem. Biophys. Res. Commun. 263*, 617−620.
36. Genetic Computer Group (1994) in *Program Manual for the Wisconsin Package*, version 8, Genetic Computer Group, Madison, WI.
37. Hodge, C. N., and Pierce, J. (1993) *Bioorg. Med. Chem. Lett. 3*, 1605−1608.
38. Jordan, D. B., and Basarab, G. S. (2000) *Bioorg. Med. Chem. Lett. 10*, 23−26.
39. Gomez, J., and Freire, E. (1995) *J. Mol. Biol. 252*, 337−350.

BI000467M